Cellular/Molecular

Voltage-Gated Sodium Channel $Na_v1.6$ Is Modulated by p38 Mitogen-Activated Protein Kinase

Ellen K. Wittmack,[1,3,4] Anthony M. Rush,[2,3,4] Andy Hudmon,[2,3,4] Stephen G. Waxman,[1,2,3,4] and Sulayman D. Dib-Hajj[2,3,4]

Departments of [1]Pharmacology and [2]Neurology and [3]The Center for Neuroscience and Regeneration Research, Yale University School of Medicine, New Haven, Connecticut 06510, and [4]Rehabilitation Research Center, Veterans Affairs Connecticut Healthcare System, West Haven, Connecticut 06516

$Na_v1.6$ is the major sodium channel isoform at nodes of Ranvier in myelinated axons and, additionally, is distributed along unmyelinated C-fibers of sensory neurons. Thus, modulation of the sodium current produced by $Na_v1.6$ might significantly impact axonal conduction. Mitogen-activated protein kinases (MAPKs) are expressed in neurons and are activated after injury, for example, after sciatic nerve transection and hypoxia. Although the role of MAPK in signal transduction and in injury-induced regulation of gene expression is well established, the ability of these kinases to phosphorylate and modulate voltage-gated sodium channels has not been reported. Sequence analysis shows that $Na_v1.6$ contains a putative MAP kinase-recognition module in the cytoplasmic loop (L1), which joins domains 1 and 2. We show in this study that sodium channels and p38 MAP kinase colocalize in rat brain tissue and that activated p38α phosphorylates L1 of $Na_v1.6$, specifically at serine 553 (S553), *in vitro*. None of the other cytoplasmic loops and termini of the channel are phosphorylated by activated p38α in these assays. Activation of p38 in the neuronal ND7/23 cell line transfected with $Na_v1.6$ leads to a significant reduction in the peak $Na_v1.6$ current amplitude, without a detectable effect on gating properties. The substitution of S553 with alanine within L1 of the $Na_v1.6$ channel prevents p38-mediated reduction of $Na_v1.6$ current density. This is the first demonstration of MAPK phosphorylation and modulation of a voltage-gated sodium channel, and this modulation may represent an additional role for MAPK in regulating the neuronal response to injury.

Key words: **protein kinase; kinase inhibitor; ion channel; patch clamp; anisomycin; stress**

Introduction

$Na_v1.6$ is the major sodium channel isoform at nodes of Ranvier (Caldwell et al., 2000; Boiko et al., 2001; Kaplan et al., 2001) and is present in the somata of small sensory neurons in dorsal root ganglion (DRG) (Black et al., 1996) and along their unmyelinated fibers within the sciatic nerve (Black et al., 2002). Recently, $Na_v1.6$ has been shown to accumulate along degenerating axons in demyelinated regions of the CNS in mice with experimental autoimmune encephalitis (EAE) and in patients with multiple sclerosis (MS) (Craner et al., 2004a,b). Additionally, $Na_v1.6$ has been shown to be significantly upregulated in activated microglia and macrophages in EAE and in acute MS lesions (Craner et al., 2005). Thus, $Na_v1.6$ appears to play an important role in normal axonal conduction and may significantly contribute to the pathophysiology of the injured nervous system.

Phosphorylation provides a fast posttranslational modification of proteins that has been shown to regulate the acute response of cells to a variety of stimuli. Although phosphorylation of sodium channels has been shown to produce rapid modulation of sodium currents, these studies have been primarily focused on investigating the role of cAMP-dependent protein kinase (PKA) and protein kinase C (PKC) (for review, see Cantrell and Catterall, 2001). However, despite the coexpression of mitogen-activated protein kinases (MAPKs) and voltage-gated sodium channels in neurons, phosphorylation and modulation of these channels by MAP kinases have not been investigated.

The four groups of MAPKs [extracellular signal-related kinase (ERK), c-Jun N-terminal kinase, p38, and ERK5/big mitogen-activated protein kinase 1] are abundant in signal transduction pathways and regulate a spectrum of processes, including inflammation, cell proliferation, differentiation, and cell death (English et al., 1999; Nebreda and Porras, 2000). Once activated, MAP kinases phosphorylate a variety of proteins and relay signals downstream, often ending in activation of transcriptional factors (Cano and Mahadevan, 1995). The four isoforms of p38 (p38α, p38β, p38γ, and p38δ) are activated by inflammatory cytokines and environmental stress (Han et al., 1994; Jiang et al., 1996, 1997; Lechner et al., 1996; Li et al., 1996; Mertens et al., 1996).

The MAPK p38α and p38β isoforms are ubiquitous, whereas p38γ is expressed prominently in muscle, and p38δ is enriched in lung and kidney (Jiang et al., 1997). CNS neurons express both $Na_v1.6$ (Schaller et al., 1995) and p38 (Jiang et al., 1996). Similarly, small DRG neurons, which include nociceptors, produce

Received Feb. 9, 2005; revised June 2, 2005; accepted June 3, 2005.

This work was supported in part by grants from the National Multiple Sclerosis Society and the Rehabilitation Research Service and Medical Research Service, Department of Veterans Affairs. E.K.W. was funded by a National Research Service Award predoctoral fellowship from the National Institute of Neurological Disorders and Stroke. The Center for Neuroscience and Regeneration Research is a Collaboration of the Paralyzed Veterans of America and the United Spinal Association with Yale University. We thank Dr. Roger Davis (University of Massachusetts Medical School, Worcester, MA) for the generous gift of the p38α plasmid and Dr. Joel Black for valuable discussions.

Correspondence should be addressed to Dr. Sulayman D. Dib-Hajj, The Center for Neuroscience and Regeneration Research, 127A, Building 34, Veterans Affairs Connecticut Healthcare System, 950 Campbell Avenue, West Haven, CT 06516. E-mail: sulayman.dib-hajj@yale.edu.

DOI:10.1523/JNEUROSCI.0541-05.2005

 0270-6474/05/256621-10$15.00/0

$Na_v1.6$ (Black et al., 1996, 2002) and p38, which is activated after inflammation (Ji et al., 2002). In addition, spinal nerve ligation causes activation of p38 in microglia of the spinal cord (Jin et al., 2003; Tsuda et al., 2004), a cell type in which $Na_v1.6$ is expressed (Craner et al., 2005). The similar tissue distribution of the two proteins suggests possible modulation of $Na_v1.6$ channels by p38. In this study, we investigated the association of MAP kinase p38 with $Na_v1.6$ in brain tissue and examined the regulation by MAP kinase p38 of the $Na_v1.6$ sodium current.

Materials and Methods

Antibodies and purified kinases. Monoclonal pan sodium channel antibody, monoclonal anti-Flag M2 antibody, and polyclonal anti-sodium channel PN4 ($Na_v1.6$) were purchased from Sigma (St. Louis, MO). The mouse anti-IgG antibody used as a control for immunoprecipitation was purchased from Vector Laboratories (Burlingame, CA). The polyclonal rabbit anti-p38 (535) antibody used for Western blot analysis and immunoprecipitation and the polyclonal goat anti-p38 antibody used for immunohistochemistry were purchased from Santa Cruz Biotechnology (Santa Cruz, CA). The secondary antibodies for Western blot analysis, anti-rabbit IgG and anti-mouse IgG, were purchased from Dako (Carpinteria, CA). The secondary antibodies used for immunohistochemistry (donkey anti-goat-AlexaFluor 488 and donkey anti-rabbit-AlexaFluor-555) were purchased from Molecular Probes (Eugene, OR). The active kinase p38α was purchased from Roche Protein Expression Group (Indianapolis, IN).

Immunohistochemistry. Immunohistochemistry was performed as described previously (Wittmack et al., 2004). Briefly, adult Sprague Dawley rats were anesthetized with ketamine and xylazine and perfused with 4% paraformaldehyde in 0.14 M Sorensen's phosphate buffer. Tissue was cryoprotected overnight at 4°C, and 10 μm sections were mounted on glass slides (Fisher SuperFrost Plus; Fisher Scientific, Houston, TX). Sections were incubated sequentially in the following: (1) blocking solution (PBS/5% normal donkey serum/2% BSA/0.1% Triton X-100/0.02% sodium azide), (2) primary antibodies [goat anti-p38, 2 μg/ml (Santa Cruz Biotechnology); rabbit anti-SCN8A ($Na_v1.6$), 3 μg/ml (Sigma)] overnight at 4°C, (3) PBS, 5×, (4) secondary antibodies (donkey anti-goat-AlexaFluor 488 and donkey anti-rabbit-AlexaFluor-555, each at 2 μg/ml) for 8 h at room temperature, and (5) PBS, 5×. Slides were coverslipped with Aqua-Poly mount, and images were obtained with a Nikon (Tokyo, Japan) E800 microscope equipped with epifluorescent optics. Images were composed in Adobe Photoshop 5.5 (Adobe Systems, San Jose, CA).

Plasmids. DNA inserts encoding the C-terminal, L1, L2, L3, and N-terminal regions of $Na_v1.6$ and the derivatives of L1 were amplified by PCR using the mouse $Na_v1.6$ plasmid (Herzog et al., 2003b) as a template. All amplicons except that of L2 were cloned in-frame into pGEX3X (Amersham Biosciences, Piscataway, NJ) at the *Bam*HI/*Eco*RI sites. L2 was cloned in-frame into the vector pGEX-4T-1 (Amersham Biosciences) at the *Eco*RI/*Xho*I sites. The plasmids were designated pGEX-$Na_v1.6$-N (amino acids 1–129), pGEX-$Na_v1.6$-L1 (amino acids 415–725), pGEX-$Na_v1.6$-L2 (amino acids 982–1193), pGEX-$Na_v1.6$-L3 (amino acids 1468–1517), and pGEX-$Na_v1.6$C (amino acids 1766–1976). Truncated derivatives of L1 were produced by inserting stop codons in pGEX-$Na_v1.6$-L1 using QuikChange XL Site-Directed Mutagenesis kit (Stratagene, La Jolla, CA). A stop codon at position 500 was introduced by changing the nucleotide cytosine in the glutamine codon (CGA) to a thymidine (TGA), thus producing the fusion protein glutathione *S*-transferase (GST)-L1A. A second mutation at amino acid 582 substituted the guanine in glutamic acid codon (GGA) by a thymidine (TGA) and created a stop codon producing the fusion protein GST-L1B. Site-directed mutagenesis was used to change serine at position 553 (S553) to an alanine, S553A in the L1B derivative, and the full-length channel (pGEX-$Na_v1.6$-L1B mutant and $Na_v1.6_R$SA). The plasmid pcDNA3-$Na_v1.6_R$, which encodes full-length mouse $Na_v1.6$, has been described previously (Herzog et al., 2003b) and contains a substitution of tyrosine 371 by serine (Y371S), which converts the $Na_v1.6$ channel sensitivity to tetrodotoxin from nanomolar to micromolar concentrations when the channel is produced in mammalian cell lines (HEK293 and ND7/23) or in DRG neurons (Herzog et al., 2003a,b; Wittmack et al., 2004; Cummins et al., 2005; Rush et al., 2005). The plasmid pCMV-Flag-p38α was a generous gift from R. Davis (University of Massachusetts Medical School, Worcester, MA). Recombinant p38 produced by this plasmid includes a Flag epitope at its N terminus.

The identities of all of the constructs were verified by sequencing of the inserts at the Howard Hughes Medical Institute/Keck Biotechnology Resource Laboratory at Yale University. Sequence analysis was performed using the basic local alignment search tool BLAST (National Library of Medicine).

Coimmunoprecipitation of sodium channels and p38. Immunoprecipitation of sodium channels and MAPK p38 was performed as described previously (Wittmack et al., 2004). Briefly, one-sixth of the cerebral hemisphere of an adult male Sprague Dawley rat was homogenized in immunoprecipitation (IP) buffer (20 mM Tris-HCl and 150 mM NaCl supplemented with protease inhibitors). Soluble proteins were extracted with 1% Triton X-100 for 15 min at 4°C and were collected in the supernatants after centrifugation at 20,000 × *g* for 20 min at 4°C. The brain lysate was precleared with protein A Sepharose beads (Amersham Biosciences). Primary antibody (2 μg; pan sodium channel or p38) was added to an equal volume of the precleared brain lysate. The antibody–brain mixture was incubated on a rotating platform at 4°C for 2 h before addition of 50 μl of preblocked protein A agarose. The mixture was incubated for 2 h at 4°C on the rotating platform. The resin complex was washed three times in 0.1% Triton X-100 in PBS and three times in PBS and denatured in 2× sample buffer at 37°C for 20 min. The proteins were separated by a 4–15% SDS-PAGE and transferred to immunoblot polyvinylidene difluoride membrane overnight at 20 V. The membrane was blocked in 10% dry milk for 1 h and incubated in primary pan sodium channel antibody (1 μg/ml) or p38 antibody (1 μg/ml) for 2 h. The membrane was then washed for 30 min and incubated with 0.1 μg/ml anti-mouse IgG (sodium channels) or 0.1 μg/ml anti-rabbit IgG (p38) for 1 h at room temperature. The membrane was washed, and the signal was detected using the ECL Plus chemiluminescent system. The *in vivo* coimmunoprecipitation experiments were each repeated three times to confirm the results.

Coimmunoprecipitation of $Na_v1.6$ and p38α from transfected HEK293 cells. The possibility of association of $Na_v1.6$ with p38α was investigated in transiently transfected HEK293 cells. HEK293 cells were cultured to 80% confluency on 10 cm dishes for 24 h and then transfected using the LipofectAMINE 2000 reagent according to the recommendations of the manufacturer (Invitrogen, Carlsbad, CA). Briefly, 12 μg of pCMV-p38α and 12 μg of pCDNA3-$Na_v1.6_R$ were added to 1.5 ml of DMEM without serum and antibiotics. In a separate tube, LipofectAMINE 2000 (60 μl) was added to 1.5 ml of DMEM (without serum and antibiotics). The two solutions were mixed together gently and incubated at room temperature for 20 min. The transfection mixture was added to the HEK293 cells, and the cells were incubated at 37°C for 24 h.

For the coimmunoprecipitation experiments, each 10 cm dish of transfected HEK293 cells was suspended in 500 μl of IP buffer, and immunoprecipitation of the protein complex by anti-p38 antibody and immunoblot assay using pan sodium channel antibody were performed as described above. Immunoblot assay of cell lysates with the anti-pan sodium channel antibody and anti-Flag antibody was used to show expression of pCMV-p38α and $Na_v1.6_R$ in the transfected cells. Each experiment was repeated three times.

Purification of GST-fusion proteins. BL21-CodonPlus-RIL competent cells (Stratagene) were transfected with constructs encoding GST-fusion proteins. A miniculture (3 ml of 2XYT media plus 100 μg/ml ampicillin) for each construct was inoculated with a single colony and allowed to grow for 4 h at 37°C. Fifty milliliter cultures of Luria broth with 100 μg/ml ampicillin were inoculated with 500 μl of the miniculture and were incubated overnight at 37°C. The next day, 500 ml cultures of 2XYT with ampicillin (100 μg/ml) were inoculated with 5 ml of the overnight culture and allowed to grow to an OD_{595} of 0.6. At this time, the cultures were cooled to 20°C and induced to produce recombinant proteins with 1 mM isopropyl-β-D-thiogalactopyranoside. The cultures were allowed to grow for an additional 4 h at 30°C, and then the bacteria were har-

vested by centrifugation at 2500 × *g* for 20 min. The cell pellets were frozen at −80°C.

The protocol for protein purification was modified from the method of Frangioni and Neel (1993). Frozen pellets were resuspended in 10 ml of ice-cold STE buffer (in mM: 10 Tris, pH 8, 1 EDTA, and 150 NaCl) with 100 μg/ml fresh lysozyme. After 15 min on ice, 5 mM DTT, protease inhibitors (benzoase nuclease at 25 U/ml), and 1.5% *N*-laurylsarcosine were added, and the bacterial lysates were sonicated and centrifuged at 10,000 × *g* for 20 min. The supernatant was isolated from the pellet, and Triton X-100 was added to a final concentration of 2%. The volume was brought up to 20 ml with STE buffer and incubated at room temperature for 30 min. The supernatant was then added to a column packed with 1.5 ml bed resin of glutathione-Sepharose beads and allowed to flow through by gravity. The columns were washed with STE buffer, and the fusion protein was eluted with GST elution buffer (in mM: 50 Tris, pH 8.0, 200 NaCl, 0.1 EDTA, and 2 DTT) with 20 mM glutathione. Protein quantification was done by Bradford assay using BSA as a standard, and the fractions containing protein were concentrated using Amicon Ultra4 (5000 molecular weight cutoff concentrators; Millipore, Bedford, MA) for 30 min at 3500 × *g*. The proteins were diluted with 1 ml of STE buffer and reconcentrated on the Amicon Ultra4 concentrator twice to reduce the glutathione in the sample before being stored in STE/10% glycerol buffer at −80°C.

Kinase assays. Kinase reactions were performed in 50 μl reactions containing 5 μl of buffer (in mM: 25 HEPES, pH 8.0, 2 DTT, and 0.1 vanadate), 5 μl of Mg/ATP (25 mM MgCl, 50 μm ATP, and 5 μCi ^{32}P-ATP), and 5 μl of substrate (protein at 1 μg/μl in 25 mM NaCl) and 35 μl of water. The purified kinase p38α was resuspended in enzyme dilution buffer (50 mM HEPES, pH 8.0, 10% glycerol, 150 mM NaCl, 0.1 mM EDTA, 0.03% NP-40, 2 mM DTT, 0.1 mM vanadate, and 1 mg/ml BSA) at a concentration of 40 ng/μl. The reaction mixture was warmed to 30°C for 2 min before the addition of 60 ng of activated p38α kinase, and the kinase reaction was allowed to proceed for an additional 5 min. A sample of the kinase reaction (25 μl) was spotted onto Whatman (Maidstone, UK) P81 paper, whereas the remainder of the kinase reaction was stopped with 2× SDS-PAGE sample buffer for gel analysis. P81 paper was washed three times with 75 mM phosphoric acid and then analyzed by a scintillation counter. For the gel electrophoresis samples, 20 μl of sample was loaded and run on a 4–15% SDS-PAGE gel. The gel was stained with Coomassie blue, destained, washed with water, and exposed to an x-ray film to visualize the phosphorylated bands. Each kinase assay was repeated three times with protein purified on three different occasions to confirm the results of the kinase experiments. ANOVA and Tukey's statistical test were run on each set of data.

Electrophysiology. Transfection of the ND7/23 cells was performed as described above with the following modifications. The cells were plated at low density on 35 mm dishes 24 h before transfection. Cells were transfected with 2 μg of $Na_v1.6_R$ and GFP, and treatment of the cells with anisomycin (Sigma) or SB203580 hydrochloride [4-(4-fluorophenyl)-2-(4-methylsulfonylphenyl)-5-(4-pyridyl)-1*H*-imidazole, HCl] (Calbiochem, La Jolla, CA), which is a specific inhibitor of MAPK p38, was performed 24 h after transfection. For the anisomycin experiments, cells were treated with 10 μg/ml anisomycin for 30 min before the culture media was replaced with the bath solution without the drug, and electrophysiological recordings were undertaken. All recordings were done within 60 min from the withdrawal of anisomycin. In the experiments with the MAPK p38 inhibitor SB203580, cells were treated with 30 μM SB203580 for 1 h preceding the recordings. In the SB203580 experiments that included anisomycin, cells were treated for 30 min with SB203580 and then 30 min with anisomycin in the continued presence of the inhibitor before recording. Data for each treatment condition were collected from at least three independent transfections.

Whole-cell voltage-clamp recordings of transfected ND7/23 cells were made using an Axopatch 200B amplifier (Axon Instruments, Union City, CA), as described previously (Wittmack et al., 2004). Only cells with a robust GFP fluorescence signal were used for recording. The pipette solution contained the following (in mM): 140 CsF, 1 EGTA, 10 NaCl, and 10 HEPES, pH 7.3 (adjusted to 310 mOsm/l with glucose). The external solution contained the following (in mM): 140 NaCl, 3 KCl, 1 $MgCl_2$, 1 $CaCl_2$, 20 tetraethylammonium-Cl, 5 CsCl, 0.1 $CdCl_2$, 10 HEPES, and 0.00025 TTX, pH 7.3 (adjusted to 320 mOsm/l with glucose). The pipette potential was adjusted to zero before seal formation, and the voltages were not corrected for liquid junction potential. Capacity transients were cancelled, and series resistance was compensated by 85–90%. Leakage current was digitally subtracted on-line using hyperpolarizing potentials applied after the test pulse (P/6 procedure). Currents were acquired using Clampex 8.1 software, filtered at 5 kHz and at a sampling rate of 20 kHz via a Digidata 1200 series interface (Axon Instruments). For current density measurements, the currents were divided by the cell capacitance, as read from the amplifier. All experiments were performed at room temperature (21–25°C). Data are expressed as mean ± SEM, and statistical analyses were performed using the Student's *t* test (significance of at least $p < 0.05$).

Voltage protocols were implemented at predetermined times from going whole cell. Briefly, standard current–voltage (*I–V*) families were obtained using 40 ms pulses from a holding potential of −120 mV, to a range of potentials (−65 to +60 mV) every 5 s. The peak value at each potential was plotted to form *I–V* curves. Activation curves were fitted with the following Boltzmann distribution equation: $G_{Na} = G_{Na,max}/(1 + \exp(V_{1/2} - V_m)/k)$, where G_{Na} is the voltage-dependent sodium conductance, $G_{Na,max}$ is the maximal sodium conductance, $V_{1/2}$ is the potential at which activation is half-maximal, V_m is the membrane potential, and k is the slope. Availability protocols consisted of a series of prepulses (−120 to +20 mV) lasting 500 ms, from the holding potential of −120 mV, followed by a 40 ms depolarization to −10 mV, every 10 s. The normalized curves were fitted using a Boltzmann distribution equation: $I_{Na}/I_{Na,max} = 1/(1 + \exp((V_m - V_{1/2})/k))$, where $I_{Na,max}$ is the peak sodium current elicited after the most hyperpolarized prepulse, V_m is the preconditioning pulse potential, $V_{1/2}$ is the half-maximal sodium current, and k is the slope factor.

Because the $Na_v1.6_R$ channel is resistant to TTX (Herzog et al., 2003b), all recordings were performed with 250 nM TTX in the bath. Endogenous TTX-sensitive (TTX-S) currents in ND7/23 are completely blocked under these conditions (Wittmack et al., 2004). Thus, the amplitude and properties of $Na_v1.6$ could be investigated without contamination by other sodium channels under the different experimental conditions in ND7/23 cells.

Results

Association of p38 and voltage-gated sodium channels in rat brain

We chose to examine the association of p38α, which is abundantly expressed in brain tissue (Jiang et al., 1996), with $Na_v1.6$ because of the ubiquitous expression pattern of $Na_v1.6$ in CNS neurons (Schaller et al., 1995). We used isoform-specific antibodies to determine whether $Na_v1.6$ and p38α are coexpressed in the same neurons. Immunohistochemical analysis shows that $Na_v1.6$ and p38α are colocalized in cerebellar Purkinje neurons (Fig. 1*A*). Coexpression of $Na_v1.6$ and p38 in the same neurons suggests the possibility that p38 can phosphorylate the channel *in vivo*.

The ability of sodium channels and p38α to form a complex in CNS tissue was investigated using coimmunoprecipitation from rat brain. Reciprocal coimmunoprecipitation experiments from rat brain lysate were done using p38 antibody to pull down sodium channels and the pan sodium channel antibody to pull down p38. Figure 1, *B* and *C*, shows a representative coimmunoprecipitation experiment from rat brain using anti-p38 antibody (*B*) and the pan sodium channel antibody (*C*). Lane 1 contains brain lysate (1/10 of the total lysate used for immunoprecipitation) as a positive control for the immunoblot assay. As expected, the control IgG antibody does not pull down immunoreactive bands of either sodium channels (Fig. 1*B*, lane 2) or MAPK p38 (Fig. 1*C*, lane 2). Lane 3 shows a sodium channel-immunoreactive band that was pulled down with the p38 antibody (*B*) and a p38-

immunoreactive band that was pulled down with the pan sodium channel antibody (*C*). The coimmunoprecipitation experiments from rat brain provide strong evidence that p38 and voltage-gated sodium channels associate *in vivo*.

$Na_v1.6$ and p38α coimmunoprecipitate from transfected HEK293 cells

Whereas the coimmunoprecipitation assay (Fig. 1*B*,*C*) shows that sodium channels and p38 form a complex, brain tissue contains multiple sodium channels in addition to $Na_v1.6$. Therefore, the ability of $Na_v1.6$ to associate specifically with p38 was investigated by a coimmunoprecipitation assay from transfected HEK293 that only produces low levels of endogenous voltage-gated sodium channels. In these experiments, HEK293 cells were transfected with either p38α or p38α plus $Na_v1.6_R$, and coimmunoprecipitation assays were performed using the p38-specific antibody. Recombinant p38 carries a Flag epitope at its N terminus, which permitted the identification of the recombinant protein in transfected cells. The immunoblot assay using the anti-Flag antibody demonstrates equal expression of the p38α protein in each transfection condition (Fig. 1*D*, bottom).

Figure 1*D* shows the results of a coimmunoprecipitation experiment from transfected HEK293 cells using a p38-specific antibody. The $Na_v1.6$ channel in the immunoprecipitated protein complex was detected using the pan sodium channel antibody, and p38 was detected using a Flag-epitope antibody. Lanes 1 and 2 show the cell lysate that was used for the coimmunoprecipitation assay, demonstrating the production of both p38 and $Na_v1.6$ in transfected cells. Lane 1 shows the presence of p38α (bottom) in cells transfected with only the kinase construct but the absence of a sodium channel immunoreactive band, consistent with the low levels of endogenous sodium channels in these cells. Lane 2 shows pan sodium channel antibody (top) and Flag-epitope antibody (bottom) -immunoreactive bands, consistent with the expression of $Na_v1.6$ (top) and p38α protein (bottom) in cells transfected with the $Na_v1.6$ and p38α constructs. Lane 3 shows the absence of a sodium channel protein in the immunoprecipitated complex from HEK293 cells transfected with only p38α. Lane 4 shows the presence of a pan sodium channel-immunoreactive band in the immunoprecipitated complex from HEK293 cells transfected with both p38α and $Nav1.6_R$. These data demonstrate that $Na_v1.6$ can associate with p38α.

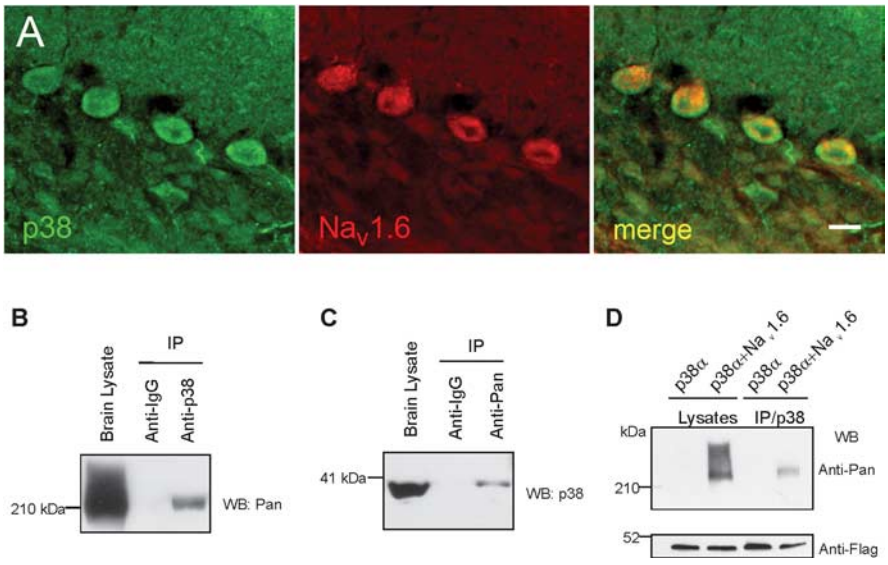

Figure 1. MAP kinase p38 associates with voltage-gated sodium channels in rat brain. ***A***, p38 (green) and $Na_v1.6$ (red) immunofluorescent signals are present within cerebellar Purkinje cells; merged image (merge) demonstrates colocalization of p38 and $Na_v1.6$ within Purkinje cells. Scale bar, 25 μm. ***B***, MAP kinase p38 antibody was used to immunoprecipitate the voltage-gated sodium channels from a rat brain lysate. Anti-mouse IgG was used as a negative control to rule out nonspecific binding. Immunoblot analysis of the IP complex was performed using pan sodium channel antibody. Lane 1 shows a robust immunoreactive signal from the cell lysate that was used for the IP assay, consistent with the presence of intact sodium channel proteins in this sample. Nonspecific antibodies do not immunoprecipitate a channel complex (lane 2). Anti-P38 coimmunoprecipitated voltage-gated sodium channels from the brain lysate (lane 3). Molecular weight marker in kilodaltons is shown on the left. ***C***, Pan sodium channel antibody was used to immunoprecipitate p38 from rat brain lysate. Anti-mouse IgG was used as a negative control to assess nonspecific binding of the channel (lane 2). Immunoblot analysis of the IP complex was done with the p38 antibody. Anti-pan sodium channel antibody immunoprecipitated p38 from rat brain lysate (lane 3). ***D***, MAPK p38 antibody was used to immunoprecipitate $Na_v1.6$ from lysates of HEK293 cells transfected with either p38α (control; lanes 1, 3) or p38α plus $Na_v1.6$ (lanes 2, 4). The IP complex was probed with the pan sodium channel antibody and detected no association between endogenous proteins with p38α (lane 3) but an association of $Na_v1.6$ with p38α (lane 4). Lanes 1 and 2 show immunoblot analysis of the cell lysates probed with pan sodium channel antibody, demonstrating comparable levels of p38α (lane 1) and $Na_v1.6$/p38α (lane 2) in the samples used for the IP assay. Immunoblot analysis using the anti-Flag antibody shows equal expression of the p38α protein (bottom). The lysate sample used as a positive control in lane 1 (***B***, ***C***) and lanes 1 and 2 (***D***) is one-tenth that used in the immunoprecipitation assays. WB, Western blot.

Intracellular loop 1 is a substrate for p38α phosphorylation

Sequence analysis of the intracellular regions of $Na_v1.6$ identified a number of serine-proline (SP) dipeptides that are putative p38 phosphorylation sites. To assess the possibility of $Na_v1.6$ phosphorylation by p38, GST-fusion proteins of the major intracellular polypeptides (GST-N, GST-L1, GST-L2, GST-L3, and GST-C) of the channel were purified from *Escherichia coli* and used as substrates in kinase assays. Kinase assays were performed using purified active p38α for 5 min at 37°C. The results of the kinase experiments are shown in Figure 2. Figure 2*A* is a schematic diagram of the sodium channel polypeptide showing the intracellular regions that were used to produce GST fusion proteins. Figure 2*B* (top) shows a Coomassie blue staining of balanced samples of the purified fusion proteins. Based on the Coomassie blue staining and Bradford determination of protein concentration, equivalent amounts of the purified GST-fusion proteins were used in the kinase assay. Figure 2*B* (bottom) shows the autoradiogram of the kinase assay. GST, GST-N, GST-L2, GST-L3, and GST-C were not phosphorylated by p38α in this assay. The L1 of $Na_v1.6$, however, is phosphorylated by p38α. L1 of $Na_v1.6$ is also phosphorylated by p38β, p38γ, and p38δ (data not shown). A histogram of the Cherenkov counts (counts per minute) for each p38 phosphorylation reaction of the different intracellular polypeptides is shown in Figure 2*C*. L1 is significantly phosphorylated (6526 $\pm$ 778 cpm) compared with GST (463 $\pm$ 136 cpm), N (635 $\pm$ 145 cpm), L2 (567 $\pm$ 70 cpm), L3 (549 $\pm$ 175 cpm), and C (498 $\pm$ 205 cpm). Statistical analysis using ANOVA and *post hoc* Tukey's test show that L1 is a good substrate for p38 compared with the other channel intracellular polypeptides ($p < 0.01$, Tukey's test) and that none of the other channel intracellular polypeptides is significantly phosphorylated above background ($p > 0.05$, Tukey's test).

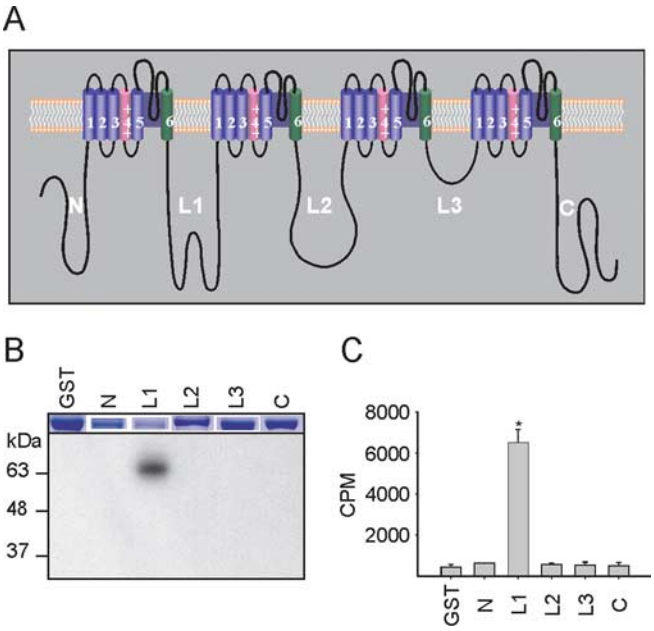

Figure 2. The first intracellular loop of $Na_v1.6$ is phosphorylated by p38α in an *in vitro* kinase assay. ***A***, Schematic of $Na_v1.6$ showing the intracellular regions that were used in the kinase assay. The N, L1, L2, L3, and C intracellular regions were produced as GST-fusion proteins. ***B***, Autoradiographic film showing phosphorylation of the L1 region of $Na_v1.6$ (top). The Coommassie blue-stained gel shows approximately equal expression of the GST-fusion proteins in the experiment. ***C***, Cherenkov counts show the relative intensity of phosphorylation of GST, N, L1, L2, L3, and C.

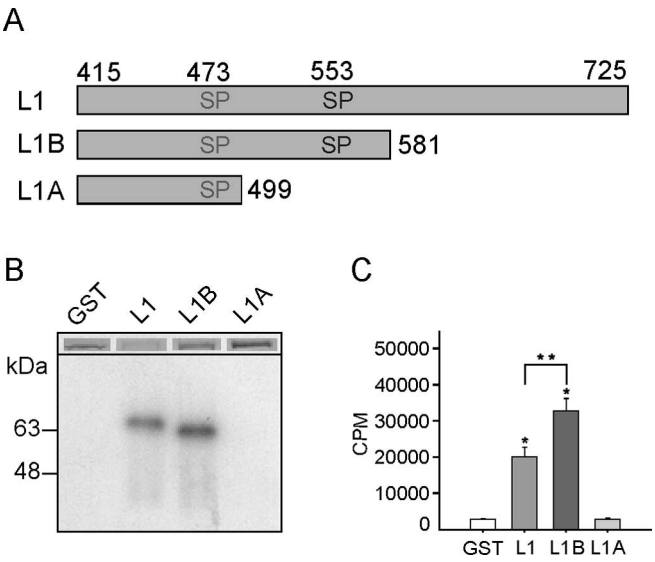

Figure 3. Deletion analysis of L1 delineates the site of p38 phosphorylation. Deletion derivatives of L1 were used to ascertain the site of p38 phosphorylation and the location of the MAPK recognition module. ***A***, Schematic of the truncations made in GST-L1. L1 is the full-length GST-L1 protein that contains proximal (473–474) and distal (553–554) SP dipeptides. L1B contains both SP dipeptides but is missing the C-terminal half of L1. L1A contains only the proximal SP dipeptide and approximately the N-terminal one-fourth of L1. ***B***, L1 and L1B are phosphorylated by p38α, but L1A is not phosphorylated. The Commassie blue-stained gel section of the figure shows equal amounts of the GST-fusion proteins used in this assay. ***C***, Histogram of the average Cherenkov counts from the phosphorylation assays shows significant ($*p < 0.01$) phosphorylation of L1 and L1B compared with GST or L1A. L1B phosphorylation is significantly higher ($**p < 0.01$) than that of L1.

Deletions in L1 of $Na_v1.6$ delineate the phosphoacceptor serine residue

Sequence analysis of L1 of $Na_v1.6$ revealed the presence of two SP dipeptides at positions 473–474 and 553–554. Additionally, MAPK recognition modules can occur on either side and distal to the phosphoacceptor residue (Sharrocks et al., 2000). To determine which of the serine residues is the phosphorylation acceptor site for p38 and to delineate the location of the putative MAPK recognition module, we derived truncated polypeptides of the L1-GST fusion protein. Site-directed mutagenesis was used to introduce stop codons into the GST-L1 construct following the amino acid residues 500 and 582, as indicated in Figure 3*A*. The GST-fusion proteins were used in p38 kinase assays as described above.

A schematic of L1 and its derivatives is shown in Figure 3*A*. The L1 construct (415–725) contains a proximal (473–474) and a distal (553–554) SP dipeptide. A stop codon was inserted at amino acid 500 to produce GST-L1A, which retains the proximal SP dipeptide, and at amino acid 582 to produce GST-L1B, which retains both SP dipeptides (473–474 and 553–554) but truncates 144 amino acids C terminal to the distal SP dipeptide.

Figure 3*B* shows the results of the kinase assay. As described above, Coomassie blue staining was used to verify that comparable amounts of fusion proteins were used in the kinase assay. GST-L1 and GST-L1B are phosphorylated by p38α, but neither GST nor GST-L1A are phosphorylated. Cherenkov counts for each reaction confirm that GST-L1 (20062 ± 2626 cpm) and GST-L1B (32742 ± 3418 cpm) are significantly different from GST (2763 ± 267 cpm) and GST-L1A (2854 ± 336 cpm) ($p < 0.01$, Tukey's test) and that GST-L1 and GST-L1B are significantly different from each other ($p < 0.01$, Tukey's test). There is no significant difference between GST and GST-L1A ($p > 0.05$, Tukey's test). These data indicate that S473 in the first SP dipeptide is not phosphorylated when L1 is truncated at position 500 but that either S473 or S553 might be phosphorylated in the full-length L1 or in a derivative, truncated at position 582. Additionally, L1B substrate produced a stronger phosphorylation signal compared with full-length L1. This could be explained by the molar excess ratio of L1B compared with L1 when equal amount of protein is used because of the smaller size of the truncated protein. Alternatively, the accessibility of the kinase to its recognition module might be enhanced by the deletion of the C-terminal half of L1.

Serine 553 is the phosphoacceptor residue in L1 of $Na_v1.6$

S553 is located 11 amino acids N terminal to the tripeptide FSF and 49 amino acids C-terminal to the sequence RKKRKQKEL, which represent a putative MAP kinase-recognition module (Sharrocks et al., 2000). To test the hypothesis that it is the serine of the distal SP dipeptide within the putative p38-binding domain of GST-L1B that is phosphorylated, S553 was changed to an alanine (S553A), as shown in the schematic in Figure 4*A*. The autoradiogram in Figure 4*B* shows that GST-L1B, but not GST-L1Bmut, is a good substrate for p38 phosphorylation. Figure 4*C* shows that the phosphorylation of GST-L1B (5868 ± 655 cpm) was more than fourfold larger than that of the GST-L1B mutant (1280 ± 236 cpm) and that this difference is significantly different from GST (534 ± 103 cpm) and GST-L1Bmut ($p < 0.01$, Tukey's test). Phosphorylation signals of GST-L1Bmut and GST were not significantly different ($p > 0.05$, Tukey's test), demonstrating that the proximal SP dipeptide (473–474) is not a good substrate for p38 kinase in this *in vitro* assay. Thus, S553 is the acceptor site in L1, which is phosphorylated by p38.

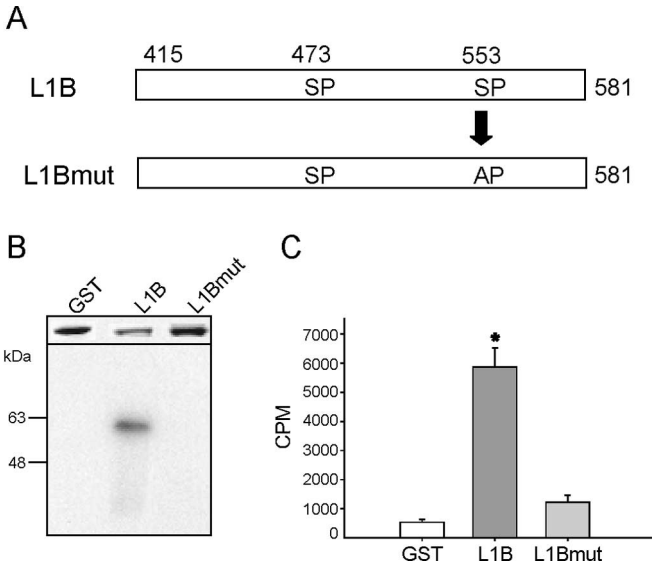

Figure 4. Serine 553 is the phosphoacceptor site in L1 for p38 MAPK. ***A***, Schematic of GST-L1B showing the substitution of the putative phosphoacceptor serine 553 by an alanine residue. ***B***, Autoradiograph showing L1B phosphorylation but not L1Bmut. Even after 24 h of developing the autoradiograph, the phosphorylation of the L1Bmut is not detectable. The Commassie blue-stained fragments above the autoradiograph show a balanced amount of GST-fusion proteins used in each assay. ***C***, Cherenkov counts from the phosphorylation experiment show significant ($*p < 0.01$) phosphorylation of L1B above GST or L1Bmut.

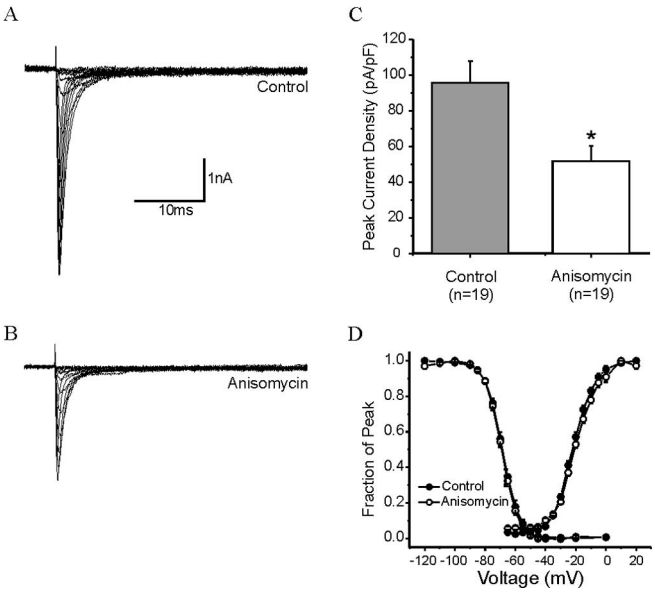

Figure 5. Anisomycin reduces peak current density of $Na_v1.6_R$. ***A***, ***B***, Representative *I–V* curve families of currents recorded in the presence of 0.25 μM TTX are shown, in which cells were depolarized to a variety of potentials (−65 to +20 mV) from a holding potential of −120 mV to elicit $Na_v1.6_R$ sodium current. Cells were treated with vehicle (DMSO) (***A***) or anisomycin (***B***) for 30 min before recording. ***C***, Peak current density (in picoamperes per picofarads) of $Na_v1.6_R$ currents showing a significant reduction with anisomycin treatment ($*p < 0.05$) compared with control. ***D***, Availability and activation curves for $Na_v1.6_R$ currents, showing no significant difference in measured biophysical properties.

Functional effects on $Na_v1.6$ currents after p38 MAPK activation

To examine the functional consequences of p38 phosphorylation of $Na_v1.6$, the sodium current properties in a neuronal cell line, ND7/23, transfected with $Na_v1.6_R$ and GFP were analyzed after treatment with anisomycin. Anisomycin is an antibiotic that is routinely used to activate p38 MAP kinases (Cano and Mahadevan, 1995). Previously, it was shown that activation of p38, as determined by the accumulation of phosphorylated p38 protein, peaks at 30 min and persists for another 30 min before it declines and disappears by 180 min (Ogawa et al., 2004). Thus, we treated cells with anisomycin for 30 min, then replaced the media with the recording bath solution without the drug, and commenced recordings for the next 60 min. We opted to activate endogenous p38 to eliminate the need to identify cells that are simultaneously triple transfected by the channel, the kinase, and the cotransfection protein marker GFP. Additionally, the activation of endogenous kinase reduces the possibility that phosphorylation of the channel is an artifact of the production of a large amount of recombinant kinase and makes the assay more similar to *in vivo* conditions.

ND7/23 cells transiently transfected with $Na_v1.6_R$ and GFP were analyzed by whole-cell voltage-clamp electrophysiology (Fig. 5). Only cells with a robust green fluorescence signal were used for electrophysiological recording. We have shown previously that all endogenous sodium currents in ND7/23 cells are blocked by 250 nM TTX (6.0 ± 0.5 pA/pF; $n = 11$) (Wittmack et al., 2004). ND7/23 cells transiently transfected with $Na_v1.6_R$ and GFP constructs produced a robust sodium current (Fig. 5*A*). Treatment of the transiently transfected ND7/23 cells by anisomycin for 30 min before recording produced a twofold decrease in current density (Fig. 5*B*,*C*), which was statistically significant ($p < 0.05$) compared with expression of $Na_v1.6_R$ and GFP without anisomycin activation. Figure 5*C* shows that cotransfection of $Na_v1.6_R$ and GFP without anisomycin produces a current density of 95 ± 12 pA/pF, whereas cotransfection of $Na_v1.6_R$ and GFP with anisomycin treatment decreases the density substantially to 52 ± 9 pA/pF ($p < 0.05$).

We also examined the effects of anisomycin on steady-state biophysical properties of $Na_v1.6_R$, and these results are shown in Figure 5*D*. The $V_{1/2}$ of voltage-dependent activation was −21.3 ± 0.8 mV ($n = 19$) under control conditions and was −19.0 ± 1.0 mV ($n = 19$) after anisomycin treatment. For channel availability, the $V_{1/2}$ of voltage dependence of inactivation was −68.6 ± 1.0 mV ($n = 12$) under control conditions and was −69.6 ± 0.8 mV ($n = 15$) after anisomycin treatment. Compared with control conditions, the voltage-dependent activation or steady-state inactivation of $Na_v1.6_R$ channels after anisomycin treatment were not significantly different ($p > 0.05$).

Although anisomycin is routinely used to activate p38 MAP kinases, this antibiotic also inhibits protein synthesis and activates other MAP kinases (Cano and Mahadevan, 1995). To confirm that the reduction in the $Na_v1.6_R$ current density is attributable to activation of p38, we used the p38-specific inhibitor SB203580 to block the effect of anisomycin treatment of transfected cells. The inactive p38 inhibitor SB202474 dihydrochloride[4-ethyl-2(*p*-methoxyphenyl)-5-(4′-pyridyl)-1*H*-imidazole, DiHCl] was used as a negative control for these experiments.

ND7/23 cells were cotransfected with GFP and $Na_v1.6_R$ and analyzed 24 h after transfection. Sister cultures were pretreated with SB203580 or the inactive counterpart SB202474 for 60 min before recording. After 30 min of SB203580 or SB202474 addition to the media, cells were treated with anisomycin for 30 min. The results of this experiment are shown in Figure 6. Treatment with the inhibitor SB203580 did not significantly change the current density of the channel (108 ± 10 pA/pF; $n = 24$; $p > 0.05$), and treatment of SB203580 followed by anisomycin blocked the decrease in the current density of the channel (110 ± 15 pA/pF;

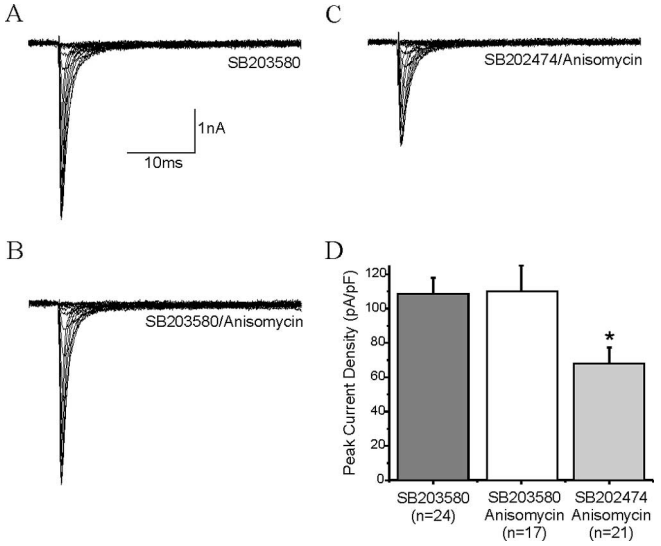

Figure 6. Reduction in peak current density by anisomycin is blocked by the specific p38 MAP kinase inhibitor SB203580. ***A–C***, Representative *I–V* curve families of currents recorded in the presence of 0.25 μM TTX are shown, in which cells were depolarized to a variety of potentials (−65 to +20 mV) from a holding potential of −120 mV to elicit $Na_v1.6_R$ sodium current. Cells were treated with the specific p38 MAP kinase inhibitor SB203580 for 60 min before recording (***A***), SB203580 for 60 min and anisomycin for 30 min (***B***), or the inactive analog SB202474 for 60 min and anisomycin for 30 min (***C***). ***D***, Peak current density (in picoamperes per picofarads) of $Na_v1.6_R$ currents, showing no significant effect of SB203580 alone ($p > 0.05$) and no reduction of current density with anisomycin treatment in the presence of SB203580 ($p > 0.05$). However, the reduction in current was still seen with anisomycin when cells were treated with the inactive analog SB202474 (*$p < 0.05$).

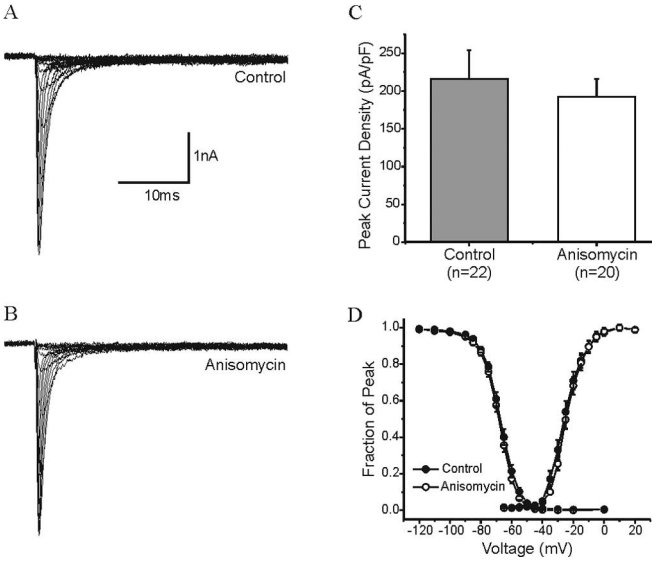

Figure 7. Reduction in $Na_v1.6$ peak current density by anisomycin is blocked by substituting serine 553 with alanine. ***A***, ***B***, Representative *I–V* curve families of currents recorded in the presence of 0.25 μM TTX are shown, in which cells were depolarized to a variety of potentials (−65 to +20 mV) from a holding potential of −120 mV to elicit $Na_v1.6_R$SA current. Cells were treated with vehicle (DMSO) (***A***) or anisomycin (***B***) for 30 min before recording. ***C***, Peak current density (in picoamperes per picofarads) of $Na_v1.6_R$SA currents showing no significant reduction with anisomycin treatment (NS) compared with control. ***D***, Availability and activation curves for $Na_v1.6_R$SA currents, showing no significant difference in measured biophysical parameters.

$n = 17$). Treatment with the inactive inhibitor SB202474, followed by anisomycin, was associated with a decrease in current density that was similar to that seen with anisomycin treatment alone (68 ± 10 pA/pF; $n = 21$; $p < 0.05$). Thus, the anisomycin-induced reduction in the $Na_v1.6_R$ current density is consistent with p38 activation and subsequent phosphorylation of the channel.

Reduction of $Na_v1.6$ current density by p38 is prevented by substituting serine 553 with alanine

The specific phosphorylation of S553 in L1 and the lack of phosphorylation of putative phosphoacceptor serine/threonine residues in L1 and the other cytoplasmic polypeptides of $Na_v1.6$ by activated p38 (Figs. 2, 4) suggested that a serine to alanine substitution (S553A) in L1 might attenuate or block the p38-mediated reduction in $Na_v1.6$ current density. S553A substitution was introduced into the $Na_v1.6_R$ construct, and the effect of anisomycin treatment of transfected ND7/23 cells was determined.

ND7/23 cells were cotransfected with GFP and $Na_v1.6_R$SA, which produced robust sodium currents (Fig. 7*A*). Treatment of the transfected ND7/23 cells by anisomycin for 30 min before recording, similar to the experiments described in Figure 5, produced no significant change in the current density (Fig. 7*B*,*C*) compared with expression of $Na_v1.6_R$SA and GFP without anisomycin treatment. Figure 7*C* shows that cotransfection of $Na_v1.6_R$SA and GFP without anisomycin treatment produces a current density of 216 ± 38 pA/pF, whereas cotransfection of $Na_v1.6_R$SA and GFP followed by anisomycin treatment produced a comparable current density of 192 ± 23 pA/pF ($p > 0.05$).

We also examined the effects of anisomycin treatment on steady-state biophysical properties of $Na_v1.6_R$SA, and these results are shown in Figure 7*D*. The $V_{1/2}$ of voltage-dependent activation was −23.2 ± 1.6 mV ($n = 22$) under control conditions and was −22.4 ± 1.5 mV ($n = 20$) after anisomycin treatment. For channel availability, the $V_{1/2}$ of voltage dependence of inactivation was −68.0 ± 1.0 mV ($n = 15$) under control conditions and −68.8 ± 0.9 ($n = 12$) after anisomycin treatment. Compared with control conditions, the voltage-dependent activation or steady-state inactivation of $Na_v1.6_R$SA channels after anisomycin treatment were not significantly different ($p > 0.05$).

Discussion

These data provide the first evidence of sodium channel modulation by a p38 MAP kinase. Our results show that $Na_v1.6$ and p38α are coexpressed in neurons *in vivo* and that sodium channels can form a complex with p38 MAP kinases in rat brain. In addition, L1 of $Na_v1.6$ appears to carry a putative p38 MAP kinase-recognition module and is phosphorylated by p38α *in vitro* at S553, nestled within this module. Electrophysiological recordings show that p38 activation reduces the current density of $Na_v1.6$ in a neuronal cell line, ND7/23, without affecting the gating properties of the channel, and that a single amino acid substitution of S553 with alanine (S553A) is sufficient to prevent the current density reduction.

Before this study, there have been a few reports on the effect of MAPK activation on ion channels, although none investigated the modulation of voltage-gated sodium currents. Activated ERK phosphorylates potassium channel $K_v4.2$ (Adams et al., 2000), causing a reduction in the A-type current produced by this channel in dendrites of hippocampal neurons (Yuan et al., 2002). Additionally, ERK-mediated reduction in the dendritic $K_v4.2$ current has been observed in temporal lobe epilepsy (Bernard et al., 2004). Constitutive phosphorylation of ERK1 and ERK2 for up to 24 h has been shown to reduce cell surface density of sodium channel $Na_v1.7$, probably attributable to the destabilization of the mRNA of the channel in adrenal chromaffin cells (Yanagita

et al., 2003). Although $Na_v1.7$ channels might have been phosphorylated under these conditions, electrophysiological recordings of sodium currents were not reported. Inflammation-induced activation of p38 in DRG neurons causes the increased translation of the vanilloid receptor TRPV1 and its selective targeting to the peripheral but not central terminals (Ji et al., 2002). It is noteworthy that the slowing of nerve conduction in diabetic neuropathy is associated with activation of p38 because treatment by the p38-specific inhibitor SB239063 restores normal nerve conduction (Price et al., 2004). The reduction in conduction velocity is consistent with previous demonstrations of slowing of nerve conduction attributable to block of sodium channels (Moore et al., 1978; Yokota et al., 1994) and with our finding that $Na_v1.6$ current density is reduced by half after p38 activation because $Na_v1.6$ is the major sodium channel isoform at nodes of Ranvier (Caldwell et al., 2000; Boiko et al., 2001; Kaplan et al., 2001) and also is present along unmyelinated fibers in the sciatic nerve (Black et al., 2002).

Kinases modulate sodium channels

Modulation of sodium channels by phosphorylation has focused primarily on the effects of PKA and PKC on these channels (Cantrell and Catterall, 2001). Sodium channels from CNS ($Na_v1.1$ and $Na_v1.2$) and peripheral nervous system ($Na_v1.7$) neurons, which are TTX-S, are phosphorylated by PKA and PKC, causing a reduction in peak sodium current by 20–50% without changing the voltage dependence of activation and inactivation (Li et al., 1992; Smith and Goldin, 1998; Vijayaragavan et al., 2004). Similarly, activation of PKC causes a reduction in peak currents of $Na_v1.2$ and $Na_v1.7$ (Cantrell et al., 2002; Vijayaragavan et al., 2004). However, PKA and PKC phosphorylation of $Na_v1.8$ produced an increase in its slow-inactivating TTX-resistant current (Gold et al., 1998; Fitzgerald et al., 1999; Vijayaragavan et al., 2004). The PKA phosphoacceptor sites S573 and S687 and the PKC phosphoacceptor site S576 in $Na_v1.2$ have been shown to be critical for the PKA- and PKC-mediated reduction in peak current amplitude (Cantrell and Catterall, 2001). The L1 sequence of $Na_v1.6$ carries a putative PKA phosphoacceptor site S561 (which corresponds to S573 in $Na_v1.2$) and a putative PKC phosphoacceptor site S563 (which corresponds to S576 of $Na_v1.2$). However, the L1 of $Na_v1.6$ lacks the equivalent of the PKA phosphoacceptor site S687 of $Na_v1.2$, which has been shown to play an important role in the modulation of $Na_v1.2$ by PKA and is conserved in $Na_v1.1$ and $Na_v1.7$. Interestingly, the equivalent of S687 is also missing from the L1 of $Na_v1.8$. Thus, it remains to be seen whether phosphorylation by PKA or PKC also reduces the current density of $Na_v1.6$ similar to $Na_v1.1$, $Na_v1.2$, and $Na_v1.7$ or increases the current density similar to $Na_v1.8$. It is reasonable to suggest that phosphorylations of different serine residues in L1 by different classes of kinases converge on a common mechanism for regulating sodium current density, possibly by controlling the binding of accessory proteins to L1.

L1 carries a putative MAPK recognition module and a site for p38 phosphorylation

Loop 1 of $Na_v1.6$ is the only cytoplasmic region of the channel that contains a putative MAP kinase-recognition module (Sharrocks et al., 2000), including the proper spacing of its components with respect to S553 (discussed below). Despite the presence of SP dipeptides in the N and C terminus of $Na_v1.6$, only L1 is phosphorylated by p38 at S553. However, it is possible that, once p38 has docked on L1 in native channels, it can phosphorylate acceptor residues of the serine/threonine proline dipeptides in other cytosolic polypeptides, which may become proximal to L1 in the folded structure of the channel. Although phosphorylation of these putative MAPK phosphoacceptor sites *in vivo* is possible, the p38-mediated reduction in current density was completely inhibited by the single amino acid substitution S553A. Thus, the phosphorylation of S553 in L1 is both necessary and sufficient to mediate the effect of p38 on $Na_v1.6$.

The presence of MAPK docking domains has been postulated to play a central role in enhancing the efficiency and accuracy of the phosphoacceptor site selection and in increasing the efficiency of phosphorylation of that residue (Sharrocks et al., 2000; Tanoue and Nishida, 2002). The L1 sequence of $Na_v1.6$ contains a string of basic residues followed by a leucine RRKKRKQKEL (residues 494–503 of mouse $Na_v1.6$), which are located 49 amino acid residues N terminal to the phosphoacceptor site S553. This sequence is similar to the docking domain for p38, which can be three to five basic residues followed by hydrophobic residues (Sharrocks et al., 2000; Tanoue and Nishida, 2002). Additionally, the tripeptide FSF (residues 566–568 of mouse $Na_v1.6$) is located 11 amino acid residues C terminal to the phoshoacceptor site in L1. The FXF motif, in which X is any amino acid residue, is typically located within 20 residues from the phosphorylated serine and is thought to either stabilize the MAPK after docking with the substrate or act together with the docking site to recruit the kinase (Sharrocks et al., 2000; Tanoue and Nishida, 2002); either way, the FXF motif enhances the specificity and efficiency of phosphorylation of the acceptor residue. The fact that all TTX-S isoforms contain a putative docking site and FXF motif with SP dipeptides nestled between them is highly suggestive of a functional role for this module in recruiting a MAPK to L1.

Functional effects of phosphorylation

MAPK p38-mediated reduction in current density could be triggered by Nedd4 ubiquitination of the channels. Nedd4 ubiquitin ligases contain multiple WW domains, which bind to proline-rich motifs (Harvey and Kumar, 1999). Nedd4-like proteins mediate a reduction of channel density of multiple voltage-gated sodium channels (Abriel et al., 2000; Fotia et al., 2004; Van Bemmelen et al., 2004; Rougier et al., 2005). This reduction has been shown to depend on the PXY motif, considered to be a WW domain class I ligand (Sudol and Hunter, 2000), in the C terminus, which is conserved in all voltage-gated sodium channels (notably including $Na_v1.6$) except $Na_v1.4$ and $Na_v1.9$. However, the motif PGSP in L1 of $Na_v1.6$ is a WW domain class IV ligand (Sudol and Hunter, 2000), which can bind Nedd4 and its related family members only when the "S" residue is phosphorylated (Lu et al., 1999; Verdecia et al., 2000; Kato et al., 2002). Thus, an Nedd4-like molecule could bind to the phosphorylated L1 of $Na_v1.6$ and ubiquinate the channel, triggering its internalization from the cell surface. Alternatively, a p38-mediated reduction of open channel probability, similar to the effect of PKA on sodium currents in cultured cortical neurons (Li et al., 1992), could also account for our findings. Additional experiments are needed to distinguish between these two mechanisms of p38 modulation of $Na_v1.6$.

The data presented here provide strong evidence for the phosphorylation and modulation of $Na_v1.6$ by p38α. More generally, the conservation of the putative MAP kinase-recognition module in multiple sodium channel isoforms might suggest a broader role for this class of kinases in modulating the electrogenic properties of neurons. Because p38 is activated after injury (Alessan-

drini et al., 1999; Sugino et al., 2000; Jin et al., 2003; Obata et al., 2004), it might be speculated that p38-mediated reduction of $Na_v1.6$ current could have adaptive value, especially after injury to CNS neurons. However, there is some evidence suggesting that suppression of p38 can rescue neurons from apoptosis and reduce neurological deficits after cerebral ischemia (Barone et al., 2001); thus, it is possible that activation of p38 after injury might amplify some pathophysiological cascades. Future studies exploring the role of MAP kinase regulation of sodium channels are crucial, given the potential adaptive and maladaptive roles that it may have in the injured nervous system.

References

Abriel H, Kamynina E, Horisberger JD, Staub O (2000) Regulation of the cardiac voltage-gated Na^+ channel (H1) by the ubiquitin-protein ligase Nedd4. FEBS Lett 466:377–380.

Adams JP, Anderson AE, Varga AW, Dineley KT, Cook RG, Pfaffinger PJ, Sweatt JD (2000) The A-type potassium channel Kv4.2 is a substrate for the mitogen-activated protein kinase ERK. J Neurochem 75:2277–2287.

Alessandrini A, Namura S, Moskowitz MA, Bonventre JV (1999) MEK1 protein kinase inhibition protects against damage resulting from focal cerebral ischemia. Proc Natl Acad Sci USA 96:12866–12869.

Barone FC, Irving EA, Ray AM, Lee JC, Kassis S, Kumar S, Badger AM, White RF, McVey MJ, Legos JJ, Erhardt JA, Nelson AH, Ohlstein EH, Hunter AJ, Ward K, Smith BR, Adams JL, Parsons AA (2001) SB 239063, a second-generation p38 mitogen-activated protein kinase inhibitor, reduces brain injury and neurological deficits in cerebral focal ischemia. J Pharmacol Exp Ther 296:312–321.

Bernard C, Anderson A, Becker A, Poolos NP, Beck H, Johnston D (2004) Acquired dendritic channelopathy in temporal lobe epilepsy. Science 305:532–535.

Black JA, Dib-Hajj S, McNabola K, Jeste S, Rizzo MA, Kocsis JD, Waxman SG (1996) Spinal sensory neurons express multiple sodium channel alpha-subunit mRNAs. Mol Brain Res 43:117–131.

Black JA, Renganathan M, Waxman SG (2002) Sodium channel $Na_v1.6$ is expressed along nonmyelinated axons and it contributes to conduction. Mol Brain Res 105:19–28.

Boiko T, Rasband MN, Levinson SR, Caldwell JH, Mandel G, Trimmer JS, Matthews G (2001) Compact myelin dictates the differential targeting of two sodium channel isoforms in the same axon. Neuron 30:91–104.

Caldwell JH, Schaller KL, Lasher RS, Peles E, Levinson SR (2000) Sodium channel $Na_v1.6$ is localized at nodes of ranvier, dendrites, and synapses. Proc Natl Acad Sci USA 97:5616–5620.

Cano E, Mahadevan LC (1995) Parallel signal processing among mammalian MAPKs. Trends Biochem Sci 20:117–122.

Cantrell AR, Catterall WA (2001) Neuromodulation of Na^+ channels: an unexpected form of cellular plasticity. Nat Rev Neurosci 2:397–407.

Cantrell AR, Tibbs VC, Yu FH, Murphy BJ, Sharp EM, Qu Y, Catterall WA, Scheuer T (2002) Molecular mechanism of convergent regulation of brain Na^+ channels by protein kinase C and protein kinase A anchored to AKAP-15. Mol Cell Neurosci 21:63–80.

Craner MJ, Hains BC, Lo AC, Black JA, Waxman SG (2004a) Co-localization of sodium channel Nav1.6 and the sodium-calcium exchanger at sites of axonal injury in the spinal cord in EAE. Brain 127:294–303.

Craner MJ, Newcombe J, Black JA, Hartle C, Cuzner ML, Waxman SG (2004b) Molecular changes in neurons in multiple sclerosis: altered axonal expression of Nav1.2 and Nav1.6 sodium channels and $Na^+/Ca2^+$ exchanger. Proc Natl Acad Sci USA 101:8168–8173.

Craner MJ, Damarjian TG, Liu S, Hains BC, Lo AC, Black JA, Newcombe J, Cuzner ML, Waxman SG (2005) Sodium channels contribute to microglia/macrophage activation and function in EAE and MS. Glia 49:220–229.

Cummins TR, Dib-Hajj SD, Herzog RI, Waxman SG (2005) $Na_v1.6$ channels generate resurgent sodium currents in spinal sensory neurons. FEBS Lett 579:2166–2170.

English J, Pearson G, Wilsbacher J, Swantek J, Karandikar M, Xu S, Cobb MH (1999) New insights into the control of MAP kinase pathways. Exp Cell Res 253:255–270.

Fitzgerald EM, Okuse K, Wood JN, Dolphin AC, Moss SJ (1999) cAMP-dependent phosphorylation of the tetrodotoxin-resistant voltage-dependent sodium channel SNS. J Physiol (Lond) 516:433–446.

Fotia AB, Ekberg J, Adams DJ, Cook DI, Poronnik P, Kumar S (2004) Regulation of neuronal voltage-gated sodium channels by the ubiquitin-protein ligases Nedd4 and Nedd4–2. J Biol Chem 279:28930–28935.

Frangioni JV, Neel BG (1993) Solubilization and purification of enzymatically active glutathione *S*-transferase (pGEX) fusion proteins. Anal Biochem 210:179–187.

Gold MS, Levine JD, Correa AM (1998) Modulation of TTX-R/(Na) by PKC and PKA and their role in PGE(2)-induced sensitization of rat sensory neurons *in vitro*. J Neurosci 18:10345–10355.

Han J, Lee JD, Bibbs L, Ulevitch RJ (1994) A MAP kinase targeted by endotoxin and hyperosmolarity in mammalian cells. Science 265:808–811.

Harvey KF, Kumar S (1999) Nedd4-like proteins: an emerging family of ubiquitin-protein ligases implicated in diverse cellular functions. Trends Cell Biol 9:166–169.

Herzog RI, Liu C, Waxman SG, Cummins TR (2003a) Calmodulin binds to the C terminus of sodium channels $Na_v1.4$ and $Na_v1.6$ and differentially modulates their functional properties. J Neurosci 23:8261–8270.

Herzog RI, Cummins TR, Ghassemi F, Dib-Hajj SD, Waxman SG (2003b) Distinct repriming and closed-state inactivation kinetics of Nav1.6 and Nav1.7 sodium channels in mouse spinal sensory neurons. J Physiol (Lond) 551:741–750.

Ji RR, Samad TA, Jin SX, Schmoll R, Woolf CJ (2002) p38 MAPK activation by NGF in primary sensory neurons after inflammation increases TRPV1 levels and maintains heat hyperalgesia. Neuron 36:57–68.

Jiang Y, Chen C, Li Z, Guo W, Gegner JA, Lin S, Han J (1996) Characterization of the structure and function of a new mitogen-activated protein kinase (p38beta). J Biol Chem 271:17920–17926.

Jiang Y, Gram H, Zhao M, New L, Gu J, Feng L, Di Padova F, Ulevitch RJ, Han J (1997) Characterization of the structure and function of the fourth member of p38 group mitogen-activated protein kinases, p38delta. J Biol Chem 272:30122–30128.

Jin SX, Zhuang ZY, Woolf CJ, Ji RR (2003) p38 mitogen-activated protein kinase is activated after a spinal nerve ligation in spinal cord microglia and dorsal root ganglion neurons and contributes to the generation of neuropathic pain. J Neurosci 23:4017–4022.

Kaplan MR, Cho M, Ullian EM, Isom LL, Levinson SR, Barres BA (2001) Differential control of clustering of the sodium channels $Na_v1.2$ and $Na_v1.6$ at developing CNS nodes of Ranvier. Neuron 30:105–119.

Kato Y, Ito M, Kawai K, Nagata K, Tanokura M (2002) Determinants of ligand specificity in groups I and IV WW domains as studied by surface plasmon resonance and model building. J Biol Chem 277:10173–10177.

Lechner C, Zahalka MA, Giot JF, Moller NP, Ullrich A (1996) ERK6, a mitogen-activated protein kinase involved in C2C12 myoblast differentiation. Proc Natl Acad Sci USA 93:4355–4359.

Li M, West JW, Lai Y, Scheuer T, Catterall WA (1992) Functional modulation of brain sodium channels by cAMP-dependent phosphorylation. Neuron 8:1151–1159.

Li Z, Jiang Y, Ulevitch RJ, Han J (1996) The primary structure of p38 gamma: a new member of p38 group of MAP kinases. Biochem Biophys Res Commun 228:334–340.

Lu PJ, Zhou XZ, Shen M, Lu KP (1999) Function of WW domains as phosphoserine- or phosphothreonine-binding modules. Science 283:1325–1328.

Mertens S, Craxton M, Goedert M (1996) SAP kinase-3, a new member of the family of mammalian stress-activated protein kinases. FEBS Lett 383:273–276.

Moore JW, Joyner RW, Brill MH, Waxman SG, Najar-Joa M (1978) Simulations of conduction in uniform myelinated fibers. Relative sensitivity to changes in nodal and internodal parameters. Biophys J 21:147–160.

Nebreda AR, Porras A (2000) p38 MAP kinases: beyond the stress response. Trends Biochem Sci 25:257–260.

Obata K, Yamanaka H, Kobayashi K, Dai Y, Mizushima T, Katsura H, Fukuoka T, Tokunaga A, Noguchi K (2004) Role of mitogen-activated protein kinase activation in injured and intact primary afferent neurons for mechanical and heat hypersensitivity after spinal nerve ligation. J Neurosci 24:10211–10222.

Ogawa T, Hayashi T, Kyoizumi S, Kusunoki Y, Nakachi K, MacPhee DG, Trosko JE, Kataoka K, Yorioka N (2004) Anisomycin downregulates gap-junctional intercellular communication via the p38 MAP-kinase pathway. J Cell Sci 117:2087–2096.

Price SA, Agthong S, Middlemas AB, Tomlinson DR (2004) Mitogen-activated protein kinase p38 mediates reduced nerve conduction velocity in experimental diabetic neuropathy: interactions with aldose reductase. Diabetes 53:1851–1856.

Rougier JS, van Bemmelen MX, Bruce MC, Jespersen T, Gavillet B, Apotheloz F, Cordonier S, Staub O, Rotin D, Abriel H (2005) Molecular determinants of voltage-gated sodium channel regulation by the Nedd4/Nedd4-like proteins. Am J Physiol Cell Physiol 288:C692–C701.

Rush AM, Dib-Hajj SD, Waxman SG (2005) Electrophysiological properties of two axonal sodium channels, Nav1.2 and Nav1.6, expressed in mouse spinal sensory neurons. J Physiol (Lond) 564:803–815.

Schaller KL, Krzemien DM, Yarowsky PJ, Krueger BK, Caldwell JH (1995) A novel, abundant sodium channel expressed in neurons and glia. J Neurosci 15:3231–3242.

Sharrocks AD, Yang SH, Galanis A (2000) Docking domains and substrate-specificity determination for MAP kinases. Trends Biochem Sci 25:448–453.

Smith RD, Goldin AL (1998) Functional analysis of the rat I sodium channel in *Xenopus* oocytes. J Neurosci 18:811–820.

Sudol M, Hunter T (2000) NeW wrinkles for an old domain. Cell 103:1001–1004.

Sugino T, Nozaki K, Takagi Y, Hattori I, Hashimoto N, Moriguchi T, Nishida E (2000) Activation of mitogen-activated protein kinases after transient forebrain ischemia in gerbil hippocampus. J Neurosci 20:4506–4514.

Tanoue T, Nishida E (2002) Docking interactions in the mitogen-activated protein kinase cascades. Pharmacol Ther 93:193–202.

Tsuda M, Mizokoshi A, Shigemoto-Mogami Y, Koizumi S, Inoue K (2004) Activation of p38 mitogen-activated protein kinase in spinal hyperactive microglia contributes to pain hypersensitivity following peripheral nerve injury. Glia 45:89–95.

Van Bemmelen MX, Rougier JS, Gavillet B, Apotheloz F, Daidie D, Tateyama M, Rivolta I, Thomas MA, Kass RS, Staub O, Abriel H (2004) Cardiac voltage-gated sodium channel Nav1.5 is regulated by Nedd4–2 mediated ubiquitination. Circ Res 95:284–291.

Verdecia MA, Bowman ME, Lu KP, Hunter T, Noel JP (2000) Structural basis for phosphoserine-proline recognition by group IV WW domains. Nat Struct Biol 7:639–643.

Vijayaragavan K, Boutjdir M, Chahine M (2004) Modulation of Nav1.7 and Nav1.8 peripheral nerve sodium channels by protein kinase A and protein kinase C. J Neurophysiol 91:1556–1569.

Wittmack EK, Rush AM, Craner MJ, Goldfarb M, Waxman SG, Dib-Hajj SD (2004) Fibroblast growth factor homologous factor 2B: association with $Na_v1.6$ and selective colocalization at nodes of Ranvier of dorsal root axons. J Neurosci 24:6765–6775.

Yanagita T, Kobayashi H, Uezono Y, Yokoo H, Sugano T, Saitoh T, Minami S, Shiraishi S, Wada A (2003) Destabilization of $Na_v1.7$ sodium channel alpha-subunit mRNA by constitutive phosphorylation of extracellular signal-regulated kinase: negative regulation of steady-state level of cell surface functional sodium channels in adrenal chromaffin cells. Mol Pharmacol 63:1125–1136.

Yokota T, Saito Y, Miyatake T (1994) Conduction slowing without conduction block of compound muscle and nerve action potentials due to sodium channel block. J Neurol Sci 124:220–224.

Yuan LL, Adams JP, Swank M, Sweatt JD, Johnston D (2002) Protein kinase modulation of dendritic K^+ channels in hippocampus involves a mitogen-activated protein kinase pathway. J Neurosci 22:4860–4868.